Theoretical Analysis of Stress and Surface Orientation Effects on Inversion Carrier Mobility

T. Ezaki, H. Nakamura, T. Yamamoto, K. Takeuchi, and M. Hane

System Devices Research Laboratories, NEC Corporation,
1120 Shimokuzawa, Sagamihara, 229-1198, Japan
t-ezaki@ap.jp.nec.com

Abstract

We performed a theoretical analysis of the stress and surface orientation effects on inversion carrier mobility modulation using a quantum mechanical carrier transport simulator that incorporates intra-valley acoustic phonons, inter-valley optical phonons, surface roughness, and impurity scattering mechanisms. The eigenstates of the inversion carrier were calculated using a pseudo-potential method with strain effects. Our simulation method successfully captures both the stress and surface orientation effects. Mobility analysis on (001) and (011) planes under $\langle 100 \rangle$ uniaxial stress revealed that tensile stress can recover (011) electron mobility to (001) surface value, and can improve hole mobility on the (011) surface.

1 Introduction

Strained silicon has attracted a great deal of attention due to its increased carrier mobility. Recently a large mobility gain was demonstrated using process induced (residual) stress [1]. Ghani's approach, however, requires different stress conditions to improve both nMOS and pMOS mobility, leading to an increased complexity in device fabrication processes. In this work, we analyzed stress-induced carrier mobility modulation, using a carrier transport simulator and taking real band structures and scattering mechanisms into account with particular focus on the surface orientation effects. The $\langle 100 \rangle$ uniaxial tensile stress increases both electron and hole mobility. Thus, it is a practical solution for lowering process complexity.

2 Simulation Method

We calculated the quantized states of the inversion carrier by using an empirical pseudo-potential method with strain effects [2, 3]. Carrier mobility was evaluated by using the relaxation time approximation, incorporating intra-valley acoustic phonons, inter-valley optical phonons, surface roughness, and ionized impurity scattering mechanisms [4]. We calculated the scattering rates with self-consistent eigen solutions of the Schrödinger and Poisson equations. The parameters related to the scattering mechanisms, such as phonon deformation potentials and the average displacement of surface roughness, were determined to reproduce carrier mobility on a (001) plane. The effective field and temperature dependencies of the inversion carrier mobility [5] were successfully captured using only one set of parameters (Fig. 1). We used the same set of scattering parameters in the following calculations.

This method can predict the current direction dependence of the carrier mobility on the (110) surface (Fig. 2) [6]. Since (001) carrier mobility is isotropic, due to the symmetry of the crystalline structure, the direction dependence is attributed to the (110) surface mobility. The current direction dependence can be explained by the energy

dispersion relationship of the quantized carrier. The peaks and valleys in hole mobility are explained by the lightest and heaviest conductivity mass, respectively [4].

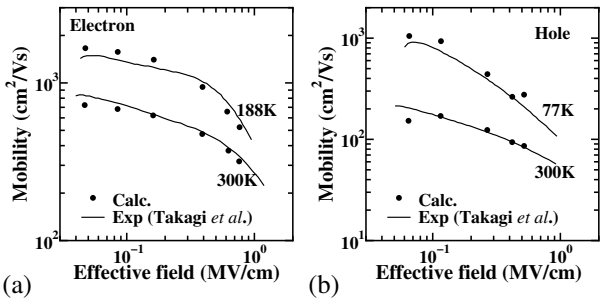

Figure 1: (a) Electron and (b) hole mobility on (001) surface orientation as a function of the effective vertical field at different temperatures. Solid circles show the simulation results; solid lines depict experimental data reported by Takagi *et al*.

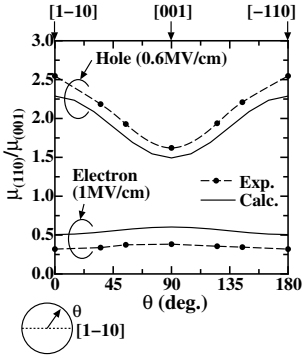

Figure 2: Electron and hole mobility on a (110) surface normalized by (001) surface mobility as a function of current direction. θ is the angle between the current and $[110]$ directions. Solid lines represent the simulation results. Solid circles with broken lines show the experimental results.

3 Results and Discussion

Our physics-based transport simulator can successfully recapture inversion carrier mobility [7–11] under biaxial stress corresponding to strained silicon on relaxed $Si_{1-x}Ge_x$ (Fig. 3). In particular, hole mobility modulation was reproduced well owing to the proper consideration of ionized impurity scattering. Stress induced mobility modulation is mostly understood through modulation of the subband energy intervals. For electrons, the energy interval between the lowest two subbands increases linearly with the germanium fraction (Fig. 4). This leads to mobility enhancement, because the intersubband phonon scattering rates decrease with the energy intervals. For the same reason, hole mobility increases as subband energy splitting increases (Fig. 3 (b)). In areas where germanium fractions are less than 0.1, however, the hole mobility remains almost unchanged, due to the small change in splitting energy.

In order to explore the possible stress conditions that enhance both electron and hole mobility together, we evaluated the inversion carrier mobility on (001) and (011) planes under $\langle 100 \rangle$ uniaxial stress conditions (Figs. 5 and 6). In these calculations, 500 MPa of compressive and tensile stress was applied, and the current flow direction was identical to the stress direction. Electron mobility under tensile stress increases by 20% and 40% for (001) and (011) surfaces, respectively (Fig. 5 (a) and (c)), relative to unstrained-case mobility on the same surface orientations. This increase is caused by the larger subband splitting, compared to the splitting in unstrained condition (Fig. 7). The tensile stress also enhances the mobility from the unstrained values (Fig. 5 (b) and (d)) on the hole. For compression, however, th electron mobility is degraded due to the decreased subband interval. Although the hole subband interval is enlarged by compressive stress, the increase in the conductivity mass cancels out the effects of subband splitting enlargement. As a result, hole mobility is not increased by the compressive

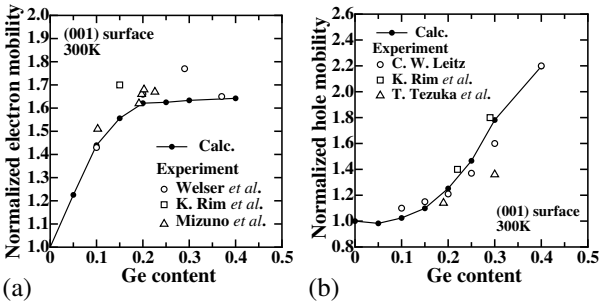

(a) (b)

Figure 3: (a) Electron and (b) hole mobility of strained silicon normalized by unstrained silicon mobility as a function of the germanium fraction. Solid lines with solid circles show the simulation results. Experimental data are shown by open symbols.

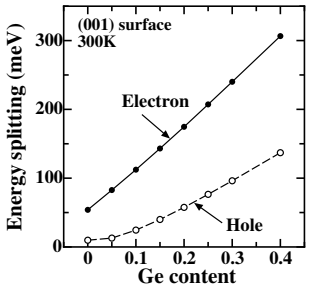

Figure 4: Energy intervals between the lowest two eigenstates as a function of the germanium fraction.

stress condition.

We found that the carrier mobility enhancement factors from unstrained (001) mobility were 20% (electron) and 15% (hole) for the (001) surface, and -10% (10% decrease for electron) and 160% (hole) for the (011) surface. As shown in Fig. 2, the electron mobility on the (011) surface is half of (001) surface mobility because of the larger conductivity mass in the (011) plane. However, the tensile stress recovers electron mobility to the value of (001) surface (Fig. 5 (c)). In particular, a large enhancement in hole mobility can be expected using the (011) surface. The tensile stress condition enhances both the electron and hole mobility on the (011) surface orientation. Therefore, a reasonable CMOS performance improvement can be obtained, even on a (011) surface, avoiding extra fabrication process complexity, such as the same strain for n- and p-MOSFETs.

4 Conclusion

We analyzed both the stress and surface orientation effects on inversion carrier mobility modulation using a newly developed quantum mechanical transport simulator that incorporates realistic band structures of quantized carriers and physics-based scattering mechanisms. Our simulator can successfully reproduce stress induced mobility modulation and surface orientation effects. This simulation method can be used to estimate stress-induced mobility enhancement. In particular, it can be used to obtain the information needed to optimize the stress conditions.

References

[1] T. Ghani *et al.*, IEDM Tech. Dig., 978 (2003).
[2] M. M. Rieger *et al.*, Phys. Rev. B **48**, 14276 (1993).
[3] H. Nakatsuji *et al.*, IEDM Tech. Dig., 727 (2002).
[4] T. Ezaki *et al.*, J. Comp. Electronics, **2**, 97 (2003).
[5] S. Takagi *et al.*, IEEE Trans. Electron Devices, **41**, 2363 (1994).
[6] H. Nakamura *et al.*, Ext. Abstracts of 2003 SSDM, 718 (2003).
[7] J. Welser *et al.*, IEDM Tech. Dig., 373 (1994).
[8] K. Rim *et al.*, IEDM Tech. Dig., 517 (1995).
[9] T. Mizuno *et al.*, 2002 VLSI Tech. Dig., 106 (2002).
[10] C. W. Leitz *et al.*, J. Appl. Phys. **92**, 3745 (2002).
[11] T. Tezuka *et al.*, Proc. 25th Int. Conf. Phys. Semicond., 1753 (2000).

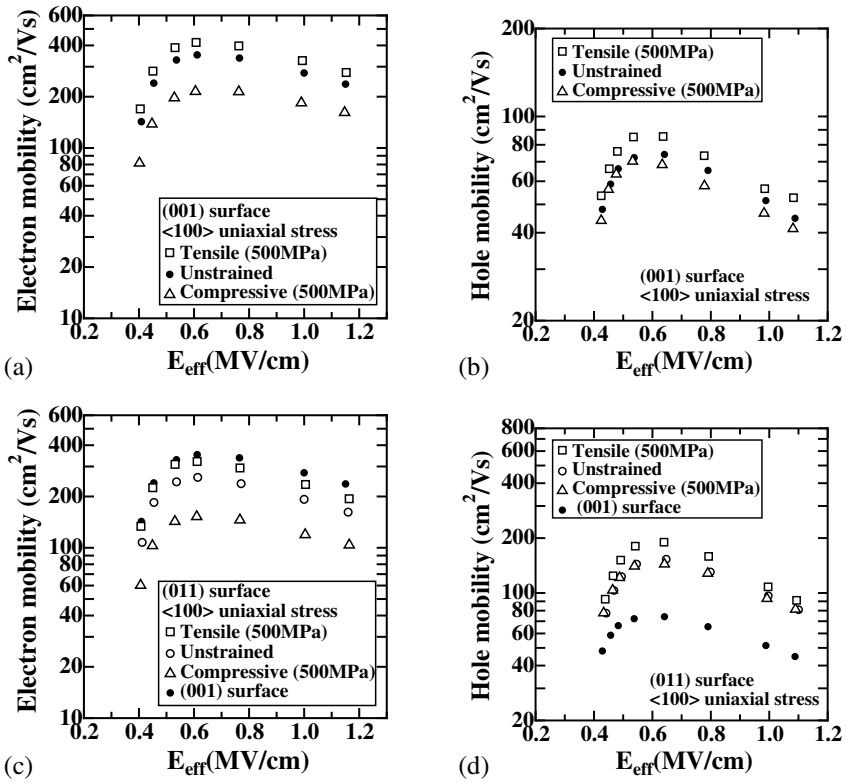

Figure 5: Simulation results of inversion electron and hole mobility on (001) and (011) surfaces under $\langle 100 \rangle$ uniaxial stress conditions. (a) and (b) are electron and hole mobility on (001) surface. (c) and (d) show electron and hole mobility on (011) surface. Open rectangles and triangles represent the mobility under tensile and compressive stress conditions, respectively. Simulation results under unstrained condition are shown by solid circles for the (001) surface and by open circles for the (011) surface.

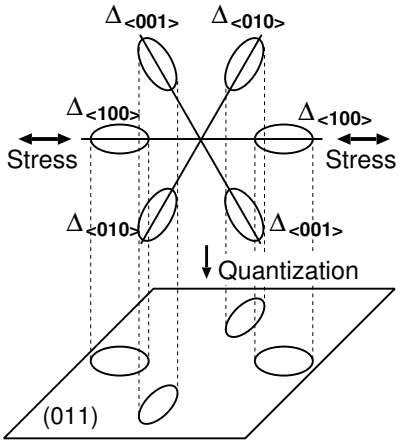

Figure 6: Schematic illustration of valleys in a conduction band, stress direction, and quantization direction for (011) surface.

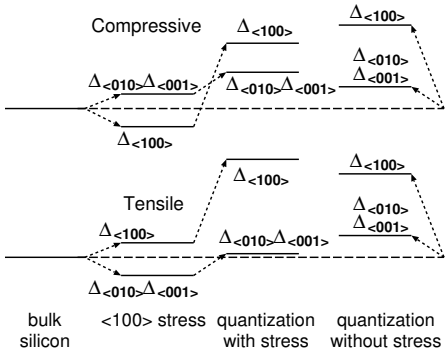

Figure 7: Energy diagram of the conduction valleys under $\langle 100 \rangle$ uniaxial stress and quantization for the (011) surface.